MKT1 alleles regulate stress responses through post-transcriptional modulation of Puf3 targets in budding yeast

Koppisetty Viswa Chaitanya[1,2] and Himanshu Sinha[1,2,3,*]

[1] Department of Biotechnology, Bhupat and Jyoti Mehta School of Biosciences, IIT Madras, Chennai 600036

[2] Centre for Integrative Biology and Systems Medicine (IBSE), IIT Madras, Chennai 600036

[3] Robert Bosch Centre for Data Science and Artificial Intelligence (RBCDSAI), IIT Madras, Chennai 600036

[*] Corresponding author: sinha@iitm.ac.in

KEYWORDS

MKT1, QTL, RNA-binding proteins, Post-transcriptional regulation, oxidative stress response

TAKE AWAY

MKT1 alleles vary stress responses by post-transcriptional modulation of Puf3 targets.

Both *PBP1* and *PUF3* contribute to the regulation of Puf3 target stability under stress.

Individual genes within the Puf3 targets have stress-specific roles in *MKT1*-mediated stress responses.

ABSTRACT

MKT1, a pleiotropic stress response gene identified by several quantitative trait studies, regulates *HO* endonuclease via the Pbp1-Pab1 complex post-transcriptionally. In addition, *MKT1*^{A89G} polymorphism was identified to contribute differentially to stress resistance. *MKT1*^{89G}, as a causal variant, determined growth advantage in multiple environments and was hypothesised to regulate differential expression during stress conditions. RNA-binding protein Puf3 modulates a set of nuclear-encoded mitochondrial transcripts whose expression was found to be affected by *MKT1* alleles. This study attempts to relate the *MKT1* allele-derived growth advantage with the stability of Puf3 targets during stress and elucidate the roles of Pbp1 and Puf3 in this mechanism. We compared the mRNA decay kinetics of a set of Puf3 targets in multiple environments to understand the allele-specific regulation by *MKT1*. Our results indicate that variation in post-transcriptional regulation between *MKT1* alleles causes this differential expression of Puf3 targets in a stress-specific manner. Additionally, *MKT1* allelic interactions with Pbp1 and Puf3 were necessary for stabilising Puf3 targets, and this regulation was specific to the *MKT1*^{89G} allele. Phenotypic analysis of these stress-specific Puf3 targets - *COX17*, *IVY1*, and *RDL2* showed that they selectively affect growth in *MKT1*^{89G} background in oxidative stress.

INTRODUCTION

The environment, with its dynamic compositional changes, poses a consistent threat to the cellular homeostatic balance (Simpson et al. 2012). Cells display an array of survival mechanisms to deal with these fluctuations by deploying environmental stress response (ESR), where the normal physiological course is transiently substituted with the synthesis of ESR-associated proteins (Lackner et al. 2012). The minimal transcription of selected genes is coupled with the suspended translation of existing transcripts. The repressed translation is followed by packing these transcripts into stress granules and translation initiation factors to serve as an energy optimisation strategy during stress (Causton et al. 2001; Buchan and Parker 2009; Buchan et al. 2011; Loll-Krippleber and Brown 2017). Cellular regulation of gene expression during stress conditions predominantly employs post-transcriptional and translational controls to modulate their synthetic activity (Lackner et al. 2012; Martínez-Salas et al. 2013).

RNA binding proteins associated with specific transcripts post-transcriptionally regulate their expression by modulating their localisation, degradation and translation (Saint-Georges et al. 2008; Martínez-Salas et al. 2013; Kechavarzi and Janga 2014; Klaus et al. 2014). Members of the Pumilio-Fem3 binding factor (PUF) family of RNA binding proteins exhibit this type of post-transcriptional regulation of sets of transcripts specific for each of five Puf protein subtypes (Olivas and Parker 2000; García-Rodríguez et al. 2007; Wang et al. 2018). Puf3 targets a module of about 220 transcripts that majorly includes nuclear-encoded mitochondrial proteins, which differ in their expression patterns during stress conditions influencing with mitochondrial biogenesis (Gerber et al. 2004; Saint-Georges et al. 2008). While utilising carbon sources that demand active respiration, the repressor-like activity of Puf3 binding to the 3'UTR elements on the transcript decreases their expression by promoting degradation or preventing it (Olivas and Parker 2000; Miller et al. 2014).

Various stress conditions, including osmotic, oxidative, nutritional deprivation, chemical, high temperature, etc., were used to understand ESR in *Saccharomyces cerevisiae* (Causton et al. 2001; Gasch and Werner-Washburne 2002; Morano et al. 2012). Studies in yeast strains from clinical and natural environments have linked genetic diversity to varying stress responses (Liti et al., 2009).

Mapping studies in segregating populations to determine causal loci for stress responses identified *MKT1*, a pleiotropic stress response gene mediating high-temperature growth (Steinmetz et al. 2002; Sinha et al. 2008), sporulation efficiency (Deutschbauer and Davis 2005), chemical stress (Ehrenreich et al. 2010) and high ethanol concentration (Swinnen et al. 2012) in different yeast strains. Besides being causal for stress responses, *MKT1* alters mitochondrial stability, affecting stress response (Dimitrov et al. 2009). At the molecular level, *MKT1* facilitates mating type switching in yeast mother cells by selective post-transcriptional regulation of *HO* endonuclease during budding. Mkt1 interaction with Pbp1, a poly-A binding protein, supports the role of Mkt1 in the post-transcriptional regulation of transcripts selectively based on the consensus sequence on 3'UTR of transcripts (Tadauchi et al. 2004). Genome-wide RNA expression analysis hypothesised that $MKT1^{A89G}$ SNP variation could be causal in altering the transcript stability of Puf3 module genes under stress conditions (Lee et al. 2009; Sun et al. 2016). Similarly, QTL coding for *IRA2* was linked to

regulating Puf4 activity and the causal polymorphisms were known to affect the transcripts encoding nucleolar ribosomal RNA-processing factors (Smith and Kruglyak 2008).

While *MKT1* as a QTL influence the Puf3 targets, another locus Pop7 positively regulates Puf3 activity (Fazlollahi et al. 2014). Additionally, overlapping targets between the Puf family proteins and the mechanism of network rewiring in the absence of Puf3 influence the expression of specific deletion phenotypes (Lapointe et al. 2017). In the current study, we link the allelic effects of *MKT1* with the stress-specific stability of Puf3 targets and elucidate the roles of *PBP1* and *PUF3* in this mechanism.

MATERIALS AND METHODS

Yeast strains and growth conditions

All the yeast strains used in the experiments are derivatives of *Saccharomyces cerevisiae*. The two parental strains used were the 'S' strain (S288c-*MKT1*^{89A}) and the 'M' strain (S288c-*MKT1*^{89G}). Strains were grown in standard YPD (1% yeast extract, 2% peptone, 2% dextrose) medium at 30°C. Plasmid-based drug cassettes amplified using pFa6A (kanMX4), pAG25 (natMx4), and pAG28 (hphMX4) as templates (Goldstein and McCusker 1999) were transformed to generate gene deletions in parental strains (Gietz et al. 1995). The stocks of H_2O_2 (H_2O_2, TCI Cat#H1222) and Cycloheximide (CYC, Sigma Cat#18079) were prepared in the water while FCCP (FCCP, TCI Cat#C3463) and 4-Nitroquinoline 1-oxide (4NQO, Sigma Cat#N8141) stocks were made in DMSO. These chemicals were added to YPD and used for stress conditions. The final concentrations used for each assay are given below.

A saturated culture from a single colony was obtained for 5ml of YPD after overnight incubation at 30°C. A dilution of 1:100 of saturated culture was used for cell counting using a haemocytometer. A serial dilution series ranging from 10^8 to 10^3 cells/ml were made for each strain. Five microliters of each dilution in the series were used to spot on YPD (control) and plates containing YPD along with stress agents (8% ethanol, 0.002% H_2O_2, 0.4µg/ml 4NQO), 0.25µg/ml CYC and 6µg/ml FCCP). The plates were incubated for four days at 30°C, following which the growth was recorded. Stress resistance was measured by comparing the number of spots with growth. All strains used for this study were diploid except for growth

kinetics experiments, which were haploid. All the strains used in this study are given in Supplementary Table 1, and the primers in Supplementary Table 2.

Growth kinetics

Turbid culture of strains in YPD was obtained in 96-well cell culture plates after 24h incubation at 30°C with 250rpm. Experiments were performed in 96-well cell culture plates, with each sample represented in triplicates of 200µl per well. Each strain was grown in YPD as a control for assays indicated with different chemicals CYC (0.1µg/ml), 4NQO (0.3µg/ml), H_2O_2 (0.01%) and FCCP (1µg/ml). The plate was incubated for 42h at 30°C at 355cpm (orbital), and OD600 was recorded every 30min using a BioTek EPOCH2 microplate reader. The growth curves were used to compute the growth rate and corresponding relative fitness. The relative fitness was defined as a ratio of the growth rate under the test condition to the growth rate in control (YPD) for the same strain.

RNA extractions

To study the temporal degradation kinetics of a candidate mRNA, 1,10-phenanthroline (Sigma Cat#131377) was used as a transcription inhibitor at a concentration of 200µg/ml in YPD and stress conditions. The overnight culture was measured at OD600 and inoculated to grow from 0.2-0.8 OD in YPD (control). For stress conditions, cultures were grown from 0.8-1.0 OD after adding stress-inducing agents to the required concentrations of CYC (3µg/ml), 4NQO (2µg/ml), H_2O_2 (0.15%), and FCCP (20µg/ml. Later 1,10-phenanthroline at 200mg/ml concentration was added to control and stress cultures. Samples were collected every 15 min after administration of the drug, for which 10ml of culture corresponding to a particular time point was spun down at 8,000 rpm for 30 sec, and the pellet was snap-frozen using liquid nitrogen.

Frozen cell pellets transferred to 1.5ml tubes were added with 50µl of Phenol-Chloroform-Isoamyl alcohol (25:24:1 ratio, PCI) (Sigma Cat#71617), 50µl of Lysis buffer (50mM Tris pH 7-7.4, 130mM NaCl, 5mM EDTA, 5% SDS) and glass beads (approximately 2/3 of the pellet volume) was added to the tube. The tubes were then vortexed at maximum speed for 20 min at 4°C, followed by centrifugation at 13,000 rpm for 15 min at 4°C. The aqueous layer was transferred to pre-cooled 0.5ml tubes, and an equal volume of PCI was added. After

vigorous mixing, the mix was centrifuged at 13,000 rpm for 10 min at 4°C. This step was repeated. The aqueous layer was extracted, and an equal volume of Chloroform-Isoamyl alcohol (24:1 ratio) was added. After vigorous mixing, the mix was centrifuged at 13,000 rpm for 10 min at 4°C. The step was repeated. The aqueous layer was removed and transferred to pre-cooled Eppendorf tubes containing 1/20th volume of 3M sodium acetate and two volumes of absolute ethanol. Total RNA was precipitated by inverting tubes and incubating them at -20°C for 30 min, followed by centrifugation at 13,000 rpm for 15 min. The pellet was washed using 200µl of 80% ethanol and centrifuged for 2 min without disrupting the pellet. The supernatant was discarded, and the pellet was air-dried on ice for 30 min.

The pellet was resuspended in a buffer containing TURBO DNase (Invitrogen Cat# 8167) following the manufacturer's instructions to remove genomic DNA contamination. The concentration of RNA in the resulting solution was measured using Nanodrop, a ratio of approximately 2.0 for 260/280 and 260/230 was considered suitable for further studies. One microgram of the sample was run on 2% agarose gel with ethidium bromide used to assess the integrity of the RNA sample.

Quantitative gene expression studies

According to the manufacturer's instructions, 3.125µg of RNA was used for cDNA synthesis using random hexamers (Invitrogen Cat#N8080127) for priming and enzyme Superscript III (Invitrogen Cat#18080093). From which 25ng of cDNA was used per qPCR reaction of 10µl using KAPA SYBR FAST (Sigma Cat# KK4618) master mix and primers. The reaction was carried out with Analytikjena qTOWER3 in a two-step cycle of denaturation at 95°C, annealing and elongation at 60°C for 35 cycles. The Ct values from the experiments were used to calculate the respective ΔCt and ΔΔCt values, which were used for further analysis.

RESULTS

***MKT1* alleles contribute differentially to growth phenotype during stress**

The phenotyping using serial dilutions (Figure 1A) showed that while in control conditions (YPD), there was no difference between the M and S strains, under stress growth conditions – ethanol, H_2O_2, FCCP, 4NQO, and CYC, the M strain grew better than the S. These phenotyping results were confirmed using haploids with growth kinetic assays where no

difference was observed between the M and S strains in YPD; in stress, the M had better growth rate and relative fitness than the S strain (Figures 1B, 1C).

The phenotypic assays of the M and S strains showed that *MKT1* was dispensable in a stress-free environment. However, the M strain had an advantage over the S strain for growth rate and relative fitness in stress conditions.

***PBP1* and *PUF3* affect the magnitude and direction of *MKT1*^{89G} mediated growth advantage during stress**

To understand the role of *PBP1* and *PUF3* in *MKT1*-mediated stress responses, *pbp1Δ*, *puf3Δ*, and *pbp1Δpuf3Δ* deletions were generated in M and S backgrounds. Growth kinetics assays in YPD showed that deleting *pbp1* or *puf3* or both had no effect in M and S backgrounds (Figure S1). Not surprisingly, the M-*pbp1Δ* strain had better relative fitness than S-*pbp1Δ* in CYC and 4NQO. However, the S-*pbp1Δ* strain showed better relative fitness than M-*pbp1Δ* in H_2O_2 and FCCP (Figure 2A).

No difference in relative growth was observed between M-*puf3Δ* and S-*puf3Δ* strains in YPD, CYC, H_2O_2, and FCCP (Figure S1). However, M-*puf3Δ* had higher relative fitness than S-*puf3Δ* in 4NQO (Figure 2B, Figure S2B).

As expected, double deletion strains of *pbp1Δpuf3Δ* in M or S backgrounds showed no growth difference in all the environments tested (Figure 2C). Thus, the double deletion of *pbp1* and *puf3* affected M and S backgrounds similarly, masking any individual allelic effects observed in the stress environments.

Analysing the *MKT1* allele and gene interactions across the environments showed that *PBP1* affected growth in CYC, and H_2O_2, while *PBP1* with *PUF3* contributed to growth in 4NQO (Figure S2). This indicated that *MKT1*-mediated stress responses could employ both *PUF3* and *PBP1* in an environment-dependent manner.

***MKT1* alleles control the expression levels of Puf3 targets using post-transcriptional machinery**

We wanted to determine the expression levels of Puf3-target and Puf3-independent genes in each environment and background (M and S, Table 1). Therefore, we analysed the

expression differences using ΔCt values of these genes at the initial time point between M and S backgrounds across multiple environments (Figure 3A).

It was observed that some of the Puf3 targets, such as *MEF1, MRPL6, PET123,* and *RSM24*, showed higher expression in M compared to the S strain across three or more environmental conditions. In YPD, even though *MKT1* alleles did not show any growth differences, a few of the Puf3-target genes *MSF1, RSM24, NAM2, MRS1,* and *MEF1* were already differentially expressed at the initial time point. However, in CYC, 4NQO, H_2O_2, and FCCP, while there was a growth difference between M and S strains, some of the Puf3-targets genes were differentially expressed between the two strains, with M allele strains showing higher expression (Figure 3A). Interestingly*, MDM10* and *FMP13* in YPD and MRC1 under CYC exhibited expression differences in non-*Puf3* targeted mitochondrial genes. Furthermore, all genes with non-mitochondrial function had no expression difference between M and S strains in YPD (Table 2). The temporal ΔCt plots of each gene for all the conditions tested were given in Supplementary Figures S3-S7.

In CYC and H_2O_2, where growth differences were observed between *MKT1* alleles, more genes were differentially expressed compared to other stress conditions. From the tested environments, including YPD, the expression levels in all the genes that showed differential expression were higher in the M compared to the S strain. This indicates that the M allele contributes to the differential expression by overexpressing some Puf3 targets in all the environments.

It has been previously shown that *MKT1* activity depends on Puf3 and Pbp1 (Tadauchi et al. 2004; Sun et al. 2016). To test if the differences described above depended on Puf3 and Pbp1, we deleted these genes in M and S backgrounds and measured expression levels at the initial time for Puf3-target genes (Figure 3B). In the *pbp1Δ* background, both in YPD and H_2O_2, for all the differentially expressed genes, the expression in M-*pbp1Δ* was higher than S-*pbp1Δ*. However, in the *puf3Δ* background, differentially expressed genes were observed in YPD alone, but interestingly, the expression of these genes was higher in the S-*puf3Δ* than in the M-*puf3Δ* strain. This is similar to the previous observations where Puf3 facilitated degradation in YPD but not under stress conditions (Miller et al. 2014). Comparison of the

results between single deletions, *pbp1Δ* and puf3Δ, and double deletion *pbp1Δpuf3Δ* backgrounds showed that the differential expression of the genes was Puf3-dependent.

To understand if this differential expression of Puf3-target genes affected their transcript stability, the transcript levels were measured at regular intervals (15 min each till 60 min endpoint) after adding 1,10-phenanthroline. The slopes of temporal ΔCt values of each Puf3-target gene in the M and S strains and in different environments were compared. This comparison was made to determine if there was a change in the stability of the transcripts of Puf3-target genes for both wild-type M and S strains in YPD and H_2O_2, Puf3-target gene slopes were highly correlated (R^2 = 0.83, p-value = 0.005) and (R^2 = 0.78, p-value = 0.013), respectively). This observation suggested that in wild-type strains, all the Puf3-target gene transcripts behaved similarly for both environments, i.e., either stabilised or degraded. For the *pbp1Δ* strain, in M and S backgrounds, Puf3-target gene slopes were only correlated in YPD (R^2 = 0.66, p-value = 0.03) and not H_2O_2. However, for the *puf3Δ* strain, in M and S backgrounds, only in H_2O_2, Puf3-target gene slopes were correlated (R^2 = 0.89, p-value = 0.0005). These results indicated that in H_2O_2, Puf3-target gene transcripts were under Pbp1 regulation.

Therefore, to check if these accessory proteins differentially altered transcript stability in an *MKT1* allele-specific manner in H_2O_2, we studied *pbp1Δ, puf3Δ and pbp1Δpuf3Δ* in the M and S backgrounds and compared transcript degradation patterns with wildtype using temporal RT-qPCR assay (Figure 4). In the wild type for YPD and H_2O_2, the median ΔΔCt was similar between M and S strains. But compared to YPD, the Puf3 targets under H_2O_2 were stabilised in both M and S strains (Figure 4A). However, in YPD and H_2O_2, between M-*pbp1Δ* and S-*pbp1Δ* strains, there was a significant difference in the rate of degradation for the majority of Puf3 gene transcripts (p-value < 10^{-3} and p-value < 10^{-3}, respectively). However, in H_2O_2, the rate of degradation of these transcripts was higher in the M-*pbp1Δ* background compared to the S-*pbp1Δ* (p-value < 4.5 x 10^{-3}) (Figure 4B). Similarly, in *puf3Δ,* the degradation rate in the M-*puf3Δ* background was higher in H_2O_2 (Figure 4C). This result indicated that Pbp1 and Puf3 were required to stabilise Puf3-target transcripts in the M background only in YPD and H_2O_2. Interestingly the double deletion *pbp1Δpuf3Δ* showed differential degradation in both YPD and H_2O_2, which was contributed by the stabilisation of M-*pbp1Δpuf3Δ* (Figure 4D). This result indicated that Pbp1 and Puf3 were required to

stabilise Puf3-target transcripts only in the M background in YPD and H_2O_2. Therefore, there was an environment-dependent stabilisation of Puf3-target genes in the M background, indicating that Pbp1 and *MKT1* alleles regulate mRNA levels post-transcriptionally.

MKT1 alleles differentially stabilise stress-specific Puf3 targets

We wanted to test whether *MKT1* alleles differentially affect the stability of Puf3 targets across the environments. Temporal mRNA samples were analysed using transcript-specific RT-qPCR assay to monitor transcript decay rates for each transcript in the M and S backgrounds and across environments. The resulting temporal ΔΔCt values of each transcript in both M and S backgrounds were compared, and Chows' test was used to determine significance. In YPD, all the genes except *HIR1, MSB3* and *MSD1* showed non-significant differences in the stability between the *MKT1* alleles. However, some Puf3-target gene transcripts showed significant variation in their stability rates between the *MKT1* alleles (Table 3). For example, in CYC, *COX17, MRS1, RDL2,* and 4NQO, *PET123, RDL2*, and *YNG2* significantly varied in their stability rates between the two *MKT1* alleles. The differentially stabilised transcripts belonged to mitochondrial and non-mitochondrial Puf3-target genes.

COX17, _RDL2_ and _IVY1_ are essential for the M strain to maintain growth advantage under oxidative stress

To determine if the differential expression of Puf3-target genes in the M strain leads to a better phenotype of the M-strain, we generated deletions of the following Puf3-target genes in both M and S strains – *COX17, IVY1, MRF1, MRS1, MSD1,* and *RDL2*. *COX17* acts as a copper metallo-chaperon in mitochondria (Heaton et al. 2000). Phospholipid-binding protein *IVY1* regulates vacuole fission (Lazar et al. 2002). *MRF1* is a mitochondrial translation release factor (Pel et al. 1992). RNA-binding protein *MRS1* controls RNA processing via splicing Group I introns in mitochondria (Kreike et al. 1986). *MSD1* is a mitochondrial aspartyl-tRNA synthetase (Gampel and Tzagoloff 1989). *RDL2* is a mitochondrial thiosulfate sulfurtransferase (Foster et al. 2009).

We grew these gene deletions in CYC, 4NQO, H_2O_2, and FCCP and compared their growth between M and S across wildtype (Figures 5A-D), *pbp1Δ* (Figures 6A-D), *puf3Δ* (Figures 7A-D), and *pbp1Δpuf3Δ* (Figures 8A-D), backgrounds. To interpret growth assay results in M and

S strains in different environmental conditions, we compared the growth of a given gene deletion in both strains. This growth difference was again compared when *puf3Δ* or *pbp1Δ* was deleted in a given gene deletion in both strains.

In CYC and 4NQO, similar to wildtype, *cox17Δ*, *ivy1Δ*, *mrs1Δ*, *msd1Δ*, and *rdl2Δ* deletions showed that M grew better than S except for *mrf1Δ*, where S was better (Figure 5A, B). In H_2O_2, while there was a difference between M and S in wild type background, the strains with the following gene deletions – *cox17Δ*, *mrs1Δ*, *mrf1Δ*, *msd1Δ* and *rdl2Δ* resulted in better fitness for M background compared to S (Figure 5C). In contrast, in FCCP, all the Puf3 target gene deletions resulted in better fitness for S background than M strains (Figure 5D, Table 4).

To understand how Pbp1 affects the phenotype of specific Puf3 target deletions we observed in the M and S backgrounds, we analysed the fitness changes in M-*pbp1Δ* and S-*pbp1Δ*. In CYC, deletion of *pbp1Δ* resulted in the loss of fitness difference between M-*pbp1Δ* and S-*pbp1Δ* strains for *cox17Δ*, *msd1Δ* and *rdl2Δ*, whereas for *ivy1Δ*, *mrf1Δ* and *mrs1Δ*, M-*pbp1Δ* grew better S-*pbp1Δ* (Figure 6A). This showed that *COX17*, *MSD1* and *RDL2* were dependent on Pbp1 in CYC. Similarly, in 4NQO, *COX17*, *IVY1*, *MSD1*, and *RDL2* were Pbp1-dependent (Figure 6B) and in H_2O_2, *COX17*, *MRS1*, *MSD1* and *RDL2* were Pbp1-dependent (Figure 6C). In FCCP, all genes except *MRS1* were Pbp1-dependent (Figure 6D). Therefore, in CYC, 4NQO, H_2O_2 and FCCP, the following genes – *COX17*, *MSD1* and *RDL2* were above *PBP1*, whereas there were a few additional genes which were environment-specific, such as *IVY1* in 4NQO and FCCP; *MRS1* in H_2O_2; *MRF1* in FCCP. This provided evidence for environment-specific regulation of Puf3-target genes by Pbp1.

Similarly, to understand the role of Puf3 over the phenotype of target gene deletions in M and S backgrounds, we analysed the fitness changes in M-*puf3Δ* and S-*puf3Δ* backgrounds. In CYC, *COX17* and *MRF1* were Puf3 dependent as their deletion led to no growth differences between M-*puf3Δ* and S-*puf3Δ* backgrounds (Figure 7A). In 4NQO, *COX17*, and *IVY1* (Figure 7B) and in H_2O_2, *COX17*, *MRF1*, *MRS1*, and *RDL2* were Puf3-dependent (Figure 7C). In FCCP, the deletion of *IVY1*, *MRF1*, *MRS1*, and *RDL2* resulted in the loss of fitness differences (Figure 7D). Together all these stress-specific genes were Puf3-dependent and were acting above Puf3 in delivering differential stress responses between *MKT1* alleles.

To resolve the influence of Pbp1 and Puf3 over the stress-specific Puf3 transcripts, we analysed the growth differences in M-*pbp1Δpuf3Δ* and S-*pbp1Δpuf3Δ* backgrounds. Based on the similarity between the individual *pbp1Δ* and *puf3Δ* backgrounds with their double deletion in CYC, *COX17* was regulated by both Pbp1 and Puf3, whereas *MRF1* was Puf3-dependent and *MSD1* and *RDL2* were Pbp1-dependent (Figure 8A). Likewise, in 4NQO, *COX17* was regulated by both Pbp1 and Puf3, while *MSD1* was Pbp1-dependent (Figure 8B). In H_2O_2, *COX17*, *MRS1*, and *RDL2* were regulated by both Pbp1 and Puf3, while *IVY1* and *MRF1* were Puf3-dependent (Figure 8C). In FCCP, *IVY1*, *MRF1*, *MSD1* and *RDL2* were regulated by both Pbp1 and Puf3, while *COX17* was Pbp1-dependent and *MRS1* was Puf3-dependent (Figure 8D). This indicates that in CYC, 4NQO and H_2O_2, the action of *COX17* depended on Pbp1 and Puf3. In addition, *MRS1* and *RDL2* in H_2O_2 and *IVY1* and *RDL2* in FCCP were other stress-specific genes depending on the action of both Pbp1 and Puf3.

DISCUSSION

Our work was based on the hypothesis that *MKT1* allele-mediated stress resistance relied on post-transcriptional modulation of mitochondrial activity via Puf3 targets. While establishing the individual roles of *PBP1* and *PUF3* as interacting genes, we attempted to provide mechanistic insights for these allelic interactions. We identified the diverse stress conditions where the wildtype M strain was consistently growing better than the S strain (Figure 1). Interestingly, Puf3 upregulated the expression of a few of its mitochondrial targets in stress conditions specific to the M strain, indicating the role of mitochondria in *MKT1* allele-specific stress resistance (Figure 4). A few of these mitochondrial target genes were observed to be crucial for the M strain exhibiting better fitness in diverse stress conditions (Figure 5). This difference in fitness was dependent on *PBP1* or *PUF3* or both in an environment-specific manner (Figures 6, 7, 8). This indicated that the role of the *MKT1* allele on fitness was both dependent on the environment and on the presence of *PBP1* and *PUF3*.

The formation of the Mkt1-Pbp1-Pab1 complex facilitates post-transcriptional regulation by Mkt1. The growth phenotype of the S strain was different from S-*pbp1Δ* in CYC and H_2O_2, indicating the formation of the Mkt1-Pbp1-Pab1 complex remains unaffected between M and S alleles under stress (Figure S2). As Pbp1 localise to stress granules regulating transcript deadenylation (Swisher and Parker 2010), this particular association allows Mkt1 to control

the stress-specific stability of mRNA. Mkt1, with its uncharacterised interaction with Puf3, was observed regulating Puf3 target degradation in an allele-specific manner. Puf3, while binding to its target mRNA, governed their access to translation machinery and was known to transiently repress nuclear-encoded mitochondrial transcripts in oxidative stress (Rowe et al. 2014). Our analysis with Puf3 target deletion strains in diverse environments confirms that the allele-specific phenotype of *MKT1* was both Pbp1 and Puf3 derived. This indicates that the ability of the M allele to stabilise stress-specific mitochondrial transcripts to modulate mitochondrial activity accounts for its better stress responses than the S allele.

The fitness advantage during stress survival was found to be dependent on $MKT1^{A89G}$ polymorphism. We observed that allele-specific alteration of Puf3 target stability leading to their elevated expression provided higher fitness for the M than the S strain. Similarly, the individual Puf3 target deletions in the M and S backgrounds were shown to determine fitness in specific environments. This indicates that the QTL variant $MKT1^{89G}$ alters mitochondrial activity via regulating stress-specific modules of Puf3 targets, compared to $MKT1^{89A}$. However, the nature of the interaction between the $MKT1^{89G}$-Pbp1-Pab1 complex and Puf3 to specify the fate of a transcript is unknown. The possible mechanisms by which the Puf target transcript can be regulated include interactions from other Puf proteins exemplified in *ZEO1* mRNA interacting with both Puf1 and Puf2 (Haramati et al. 2017), facilitating mRNA degradation by promoting deadenylation (Olivas and Parker 2000) and mRNA localisation to mitochondria via Mdm12 and Tom20 (Miller et al. 2014). Our results highlight another level of regulatory complexity where coding polymorphisms in QTL, like *MKT1*, can modulate multiple stress responses through post-transcriptional control.

ACKNOWLEDGEMENTS

The authors acknowledge help from Rajeeva Lokshanan in the statistical analysis of some of the data. The authors thank K Subramanian for critically reading the manuscript and comments. VCK acknowledges the University Grant Commission Junior Research Fellowship. HS acknowledges intra-mural funding from IIT Madras and Excelra Knowledge Solutions Pvt. Ltd. (CR/22-23/0026/BT/EXCE/008752).

AUTHOR CONTRIBUTIONS

VCK and HS designed all the experiments, VCK performed all the experiments, and VCK and HS wrote the manuscript.

CONFLICT OF INTEREST

The authors declare that they have no competing interests.

REFERENCES

Buchan JR, Yoon JH, Parker R. Stress-specific composition, assembly and kinetics of stress granules in *Saccharomyces cerevisiae*. *J Cell Sci*. 2011; 124(Pt 2):228-239. doi:10.1242/jcs.078444

Buchan JR, Parker R. Eukaryotic stress granules: the ins and outs of translation. *Mol Cell*. 2009; 36(6):932-941. doi:10.1016/j.molcel.2009.11.020

Causton HC, Ren B, Koh SS, et al. Remodeling of yeast genome expression in response to environmental changes. *Mol Biol Cell*. 2001; 12(2):323-337. doi:10.1091/mbc.12.2.323

Deutschbauer AM, Davis RW. Quantitative trait loci mapped to single-nucleotide resolution in yeast. *Nat Genet*. 2005; 37(12):1333-1340. doi:10.1038/ng1674

Dimitrov LN, Brem RB, Kruglyak L, Gottschling DE. Polymorphisms in multiple genes contribute to the spontaneous mitochondrial genome instability of *Saccharomyces cerevisiae* S288c strains. *Genetics*. 2009; 183(1):365-383. doi:10.1534/genetics.109.104497

Ehrenreich IM, Torabi N, Jia Y, et al. Dissection of genetically complex traits with extremely large pools of yeast segregants. *Nature*. 2010; 464(7291):1039-1042. doi:10.1038/nature08923

Fazlollahi M, Lee E, Muroff I, et al. Harnessing natural sequence variation to dissect posttranscriptional regulatory networks in yeast. *G3 (Bethesda)*. 2014; 4(8):1539-1553. doi:10.1534/g3.114.012039

Foster MW, Forrester MT, Stamler JS. A protein microarray-based analysis of S-nitrosylation. *Proc Natl Acad Sci U S A*. 2009; 106(45):18948-18953. doi:10.1073/pnas.0900729106

Gampel A, Tzagoloff A. Homology of aspartyl- and lysyl-tRNA synthetases. *Proc Natl Acad Sci U S A*. 1989; 86(16):6023-6027. doi:10.1073/pnas.86.16.6023

García-Rodríguez LJ, Gay AC, Pon LA. Puf3p, a Pumilio family RNA binding protein, localizes to mitochondria and regulates mitochondrial biogenesis and motility in budding yeast. *J Cell Biol*. 2007; 176(2):197-207. doi:10.1083/jcb.200606054

Gasch AP, Werner-Washburne M. The genomics of yeast responses to environmental stress and starvation. *Funct Integr Genomics*. 2002; 2(4-5):181-192. doi:10.1007/s10142-002-0058-2

Gerber AP, Herschlag D, Brown PO. Extensive association of functionally and cytotopically related mRNAs with Puf family RNA-binding proteins in yeast. *PLoS Biol*. 2004; 2(3):E79. doi:10.1371/journal.pbio.0020079

Gietz RD, Schiestl RH, Willems AR, Woods RA. Studies on the transformation of intact yeast cells by the LiAc/SS-DNA/PEG procedure. *Yeast*. 1995; 11(4):355-360. doi:10.1002/yea.320110408

Goldstein AL, McCusker JH. Three new dominant drug resistance cassettes for gene disruption in *Saccharomyces cerevisiae*. *Yeast*. 1999; 15(14):1541-1553.

Gupta I, Clauder-Münster S, Klaus B, et al. Alternative polyadenylation diversifies post-transcriptional regulation by selective RNA-protein interactions. *Mol Syst Biol*. 2014; 10(2):719. doi:10.1002/msb.135068

Haramati O, Brodov A, Yelin I, Atir-Lande A, Samra N, Arava Y. Identification and characterization of roles for Puf1 and Puf2 proteins in the yeast response to high calcium. *Sci Rep*. 2017; 7(1):3037. doi:10.1038/s41598-017-02873-z

Heaton D, Nittis T, Srinivasan C, Winge DR. Mutational analysis of the mitochondrial copper metallochaperone Cox17. *J Biol Chem*. 2000; 275(48):37582-37587. doi:10.1074/jbc.M006639200

Huang YF, Doligez A, Fournier-Level A, et al. Dissecting genetic architecture of grape proanthocyanidin composition through quantitative trait locus mapping. *BMC Plant Biol*. 2012; 12(1):30. doi:10.1186/1471-2229-12-30

Kechavarzi B, Janga SC. Dissecting the expression landscape of RNA-binding proteins in human cancers. *Genome Biol*. 2014; 15(1):R14. doi:10.1186/gb-2014-15-1-r14

Kreike J, Schulze M, Pillar T, Körte A, Rödel G. Cloning of a nuclear gene MRS1 involved in the excision of a single group I intron (bI3) from the mitochondrial COB transcript in *S. cerevisiae*. *Curr Genet*. 1986; 11(3):185-191. doi:10.1007/bf00420605

Lackner DH, Schmidt MW, Wu S, Wolf DA, Bähler J. Regulation of transcriptome, translation, and proteome in response to environmental stress in fission yeast. *Genome Biol*. 2012; 13(4):R25. doi:10.1186/gb-2012-13-4-r25

Lapointe CP, Preston MA, Wilinski D, Saunders HAJ, Campbell ZT, Wickens M. Architecture and dynamics of overlapped RNA regulatory networks. *RNA*. 2017; 23(11):1636-1647. doi:10.1261/rna.062687.117

Lazar T, Scheglmann D, Gallwitz D. A novel phospholipid-binding protein from the yeast *Saccharomyces cerevisiae* with dual binding specificities for the transport GTPase Ypt7p and the Sec1-related Vps33p. *Eur J Cell Biol*. 2002; 81(12):635-646. doi:10.1078/0171-9335-00290

Lee SI, Dudley AM, Drubin D, et al. Learning a prior on regulatory potential from eQTL data. *PLoS Genet*. 2009; 5(1):e1000358. doi:10.1371/journal.pgen.1000358

Liti G, Carter DM, Moses AM, et al. Population genomics of domestic and wild yeasts. *Nature*. 2009; 458(7236):337-341. doi:10.1038/nature07743

Loll-Krippleber R, Brown GW. P-body proteins regulate transcriptional rewiring to promote DNA replication stress resistance. *Nat Commun*. 2017; 8(1):558. doi:10.1038/s41467-017-00632-2

Martínez-Salas E, Lozano G, Fernandez-Chamorro J, Francisco-Velilla R, Galan A, Diaz R. RNA-binding proteins impacting on internal initiation of translation. *Int J Mol Sci*. 2013; 14(11):21705-21726. doi:10.3390/ijms141121705

Miller MA, Russo J, Fischer AD, Lopez Leban FA, Olivas WM. Carbon source-dependent alteration of Puf3p activity mediates rapid changes in the stabilities of mRNAs involved in mitochondrial function. *Nucleic Acids Res*. 2014; 42(6):3954-3970. doi:10.1093/nar/gkt1346

Morano KA, Grant CM, Moye-Rowley WS. The response to heat shock and oxidative stress in *Saccharomyces cerevisiae*. *Genetics*. 2012; 190(4):1157-1195. doi:10.1534/genetics.111.128033

Olivas W, Parker R. The Puf3 protein is a transcript-specific regulator of mRNA degradation in yeast. *EMBO J*. 2000; 19(23):6602-6611. doi:10.1093/emboj/19.23.6602

Pel HJ, Maat C, Rep M, Grivell LA. The yeast nuclear gene *MRF1* encodes a mitochondrial peptide chain release factor and cures several mitochondrial RNA splicing defects. *Nucleic Acids Res*. 1992; 20(23):6339-6346. doi:10.1093/nar/20.23.6339

Rowe W, Kershaw CJ, Castelli LM, et al. Puf3p induces translational repression of genes linked to oxidative stress. *Nucleic Acids Res*. 2014; 42(2):1026-1041. doi:10.1093/nar/gkt948

Saint-Georges Y, Garcia M, Delaveau T, et al. Yeast mitochondrial biogenesis: a role for the PUF RNA-binding protein Puf3p in mRNA localization. *PLoS One*. 2008; 3(6):e2293. doi:10.1371/journal.pone.0002293

Simpson CE, Ashe MP. Adaptation to stress in yeast: to translate or not? *Biochem Soc Trans*. 2012; 40(4):794-799. doi:10.1042/bst20120078

Sinha H, David L, Pascon RC, et al. Sequential elimination of major-effect contributors identifies additional quantitative trait loci conditioning high-temperature growth in yeast. *Genetics*. 2008; 180(3):1661-1670. doi:10.1534/genetics.108.092932

Smith EN, Kruglyak L. Gene-environment interaction in yeast gene expression. *PLoS Biol*. 2008; 6(4):e83. doi:10.1371/journal.pbio.0060083

Steinmetz LM, Sinha H, Richards DR, et al. Dissecting the architecture of a quantitative trait locus in yeast. *Nature*. 2002; 416(6878):326-330. doi:10.1038/416326a

Sun X, Wang Z, Guo X, Li H, Gu Z. Coordinated evolution of transcriptional and post-transcriptional regulation for mitochondrial functions in yeast strains. *PLoS One*. 2016; 11(4):e0153523. doi:10.1371/journal.pone.0153523

Swinnen S, Schaerlaekens K, Pais T, et al. Identification of novel causative genes determining the complex trait of high ethanol tolerance in yeast using pooled-segregant whole-genome sequence analysis. *Genome Res*. 2012;22(5):975-984. doi:10.1101/gr.131698.111

Swisher KD, Parker R. Localization to, and effects of Pbp1, Pbp4, Lsm12, Dhh1, and Pab1 on stress granules in *Saccharomyces cerevisiae*. *PLoS One*. 2010; 5(4):e10006. doi:10.1371/journal.pone.0010006

Tadauchi T, Inada T, Matsumoto K, Irie K. Posttranscriptional regulation of *HO* expression by the Mkt1-Pbp1 complex. *Mol Cell Biol*. 2004; 24(9):3670-3681. doi:10.1128/MCB.24.9.3670-3681.2004

Wang M, Ogé L, Perez-Garcia MD, Hamama L, Sakr S. The PUF protein family: Overview on PUF RNA targets, biological functions, and post transcriptional regulation. *Int J Mol Sci*. 2018; 19(2). doi:10.3390/ijms19020410

TABLES

Table 1: List of genes analysed using RT-qPCR studies.

Puf3 affinity	**Function**	**Gene**
Puf3 targets	Mitochondrial	*ARG2, COX17, MEF1, MRF1, MRPL6, MRS1, MSD1, MSF1, MSS2, NAM2, PET123, RDL2, RSM24, SUV3, TIM44*
	Non-mitochondrial	*CCC2, CTM1, HIR1, HOT1, IVY1, KEL2, MSB3, UBP16, YNG2*
Non-Puf3 targets	Mitochondrial	*ECM10, RNR3*

Table 2: List of genes showing differential expression of transcripts between M and S strains under each growth condition.

Environment	**Puf3 targets showing differential degradation**
YPD	*MEF1, MRPL6, MRS1, MSF1, NAM2, PET123, RSM24*
CYC	*MRPL6, PET123, CTM1, HOT1, KEL2, UBP16*
4NQO	*PET123, RSM24, SUV3*
H_2O_2	*COX17, MEF1, MRF1, MRPL6, MSS2, NAM2, RSM24, UBP16, YNG2*
FCCP	*MEF1, PET123, RSM24, CTM1*

Table 3: List of genes showing differential degradation of transcripts between M and S strains under each growth condition.

Environment	Genes showing differential degradation	
	Puf3 targets	**Non-Puf3 targets**
YPD	*HIR1, MSB3, MSD1*	
CYC	*COX17, MRS1, RDL2,*	*RNR3*
4NQO	*PET123, RDL2, YNG2*	
H_2O_2	*RSM24*	
FCCP	*PET123, SUV3*	*RNR3*

Table 4: List of gene deletions differing with wildtype growth phenotype in each growth environment.

Environment	Gene deletion differing from wildtype
CYC	*mrf1Δ*
4NQO	*mrf1Δ*
H_2O_2	*cox17Δ, mrs1Δ, mrf1Δ, msd1Δ, rdl2Δ*
FCCP	*cox17Δ, ivy1Δ, mrf1Δ, mrs1Δ, msd1Δ, rdl2Δ*

FIGURE LEGENDS

Figure 1: Analysis of *MKT1* allelic variants for pleiotropic stress resistance. [A] 10-fold serial dilution ranging from 10^8-10^3 cells/ml of S and M strains were spotted on YPD, 8% ethanol, 0.002% H_2O_2, 0.4µg/ml 4NQO, 0.25µg/ml CYC and 6µg/ml FCCP. Comparison of [B] growth rates and [C] relative fitness between M and S strains across YPD, 0.1µg/ml CYC, 0.3µg/ml 4NQO, 0.01% H_2O_2 and 1µg/ml FCCP. The experiments were performed in triplicates, and the error bars represent SD. P-values were calculated using a t-test, and significance was indicated as non-significant (ns), $p < 0.05$(*), < 0.001(**), < 0.0001(***) and < 0.00001(****) on the top of each comparison.

Figure 2: Role of *PBP1* and *PUF3* in *MKT1*-mediated stress responses. Relative fitness between M and S backgrounds with [A] *pbp1Δ*, [B] *puf3Δ* and [C] *pbp1Δpuf3Δ* deletions across YPD, 0.1µg/ml CYC, 0.3µg/ml 4NQO, 0.01% H_2O_2 and 1µg/ml FCCP. The experiments were performed in triplicates, and the error bars represent SD. P-values were calculated using a t-test, and significance was indicated as non-significant (ns), $p < 0.05$(*), < 0.001(**), < 0.0001(***), and < 0.00001(****) on the top of each comparison.

Figure 3: Differential expression (ΔCt) of Puf3 targets between M and S backgrounds at initial time point [A] wildtype across multiple environments, [B] *pbp1Δ*, *puf3Δ* and *pbp1Δpuf3Δ* deletions across YPD and H_2O_2. Cells were grown in YPD (control), CYC (3µg/ml), 4NQO (2µg/ml), H_2O_2 (0.15%) and FCCP (20µg/ml). The experiments were performed in triplicates, and the significant differences ($p < 0.05$) in ΔCt between M and S backgrounds were reported.

Figure 4: Analysis of temporal median ΔΔCt values among Puf3 targets between M and S backgrounds in [A] wildtype [B] *pbp1Δ*, [C] *puf3Δ* and [D] *pbp1Δpuf3Δ* deletions across YPD and H_2O_2 (0.15%). The experiments were performed in triplicates, and the error bars represent SD. P-values were calculated using a t-test, and significance was indicated as non-significant (ns), $p < 0.05$ (*), < 0.001 (**), < 0.0001 (***), and < 0.00001 (****) on the top of each comparison.

Figure 5: Stress-specific roles of Puf3 targets. Comparison of relative fitness between M and S backgrounds with the deletion of Puf3 targets *COX17*, *IVY1*, *MRF1*, *MRS1*, *MSD1*, and *RDL2* in wildtype across [A] 0.1µg/ml CYC, [B] 0.3µg/ml 4NQO, [C] 0.01% H_2O_2 and [D] 1µg/ml FCCP. The experiments were performed in triplicates, and the error bars represent SD. P-values were calculated using a t-test, and significance was indicated as non-significant (ns), $p < 0.05$ (*), 0.001 (**), 0.0001 (***) and 0.00001 (****) on the top of each comparison.

Figure 6: Effect Pbp1 on Puf3 target deletion phenotype. Comparison of relative fitness between M and S backgrounds with the deletion of Puf3 targets *COX17*, *IVY1*, *MRF1*, *MRS1*, *MSD1*, and *RDL2* in *pbp1Δ* background across [A] 0.1µg/ml CYC, [B] 0.3µg/ml 4NQO, [C] 0.01% H_2O_2 and [D] 1µg/ml FCCP. The experiments were performed in triplicates, and the error bars represent SD. P-values were calculated using a t-test, and significance was indicated as non-significant (ns), $p < 0.05$ (*), 0.001(**), 0.0001 (***) and 0.00001 (****) on the top of each comparison.

Figure 7: Effect Puf3 on Puf3 target deletion phenotype. Comparison of relative fitness between M and S backgrounds with the deletion of Puf3 targets *COX17*, *IVY1*, *MRF1*, *MRS1*, *MSD1*, and *RDL2* in *puf3Δ* background across [A] 0.1µg/ml CYC, [B] 0.3µg/ml 4NQO, [C] 0.01% H_2O_2 and [D] 1µg/ml FCCP. The experiments were performed in triplicates, and the error bars represent SD. P-values were calculated using a t-test, and significance was indicated as non-significant (ns), $p <0.05$ (*), 0.001 (**), 0.0001 (***) and 0.00001 (****) on the top of each comparison.

Figure 8: Effect Pbp1 and Puf3 on Puf3 target deletion phenotype. Comparison of relative fitness between M and S backgrounds with the deletion of Puf3 targets *COX17*, *IVY1*, *MRF1*, *MRS1*, *MSD1*, and *RDL2* in *pbp1Δpuf3Δ* background across [A] 0.1µg/ml CYC, [B] 0.3µg/ml 4NQO, [C] 0.01% H_2O_2 and [D] 1µg/ml FCCP. The experiments were performed in triplicates, and the error bars represent SD. P-values were calculated using a t-test, and significance was indicated as non-significant (ns), $p < 0.05$ (*), 0.001 (**), 0.0001 (***) and 0.00001 (****) on the top of each comparison.

Figure 1

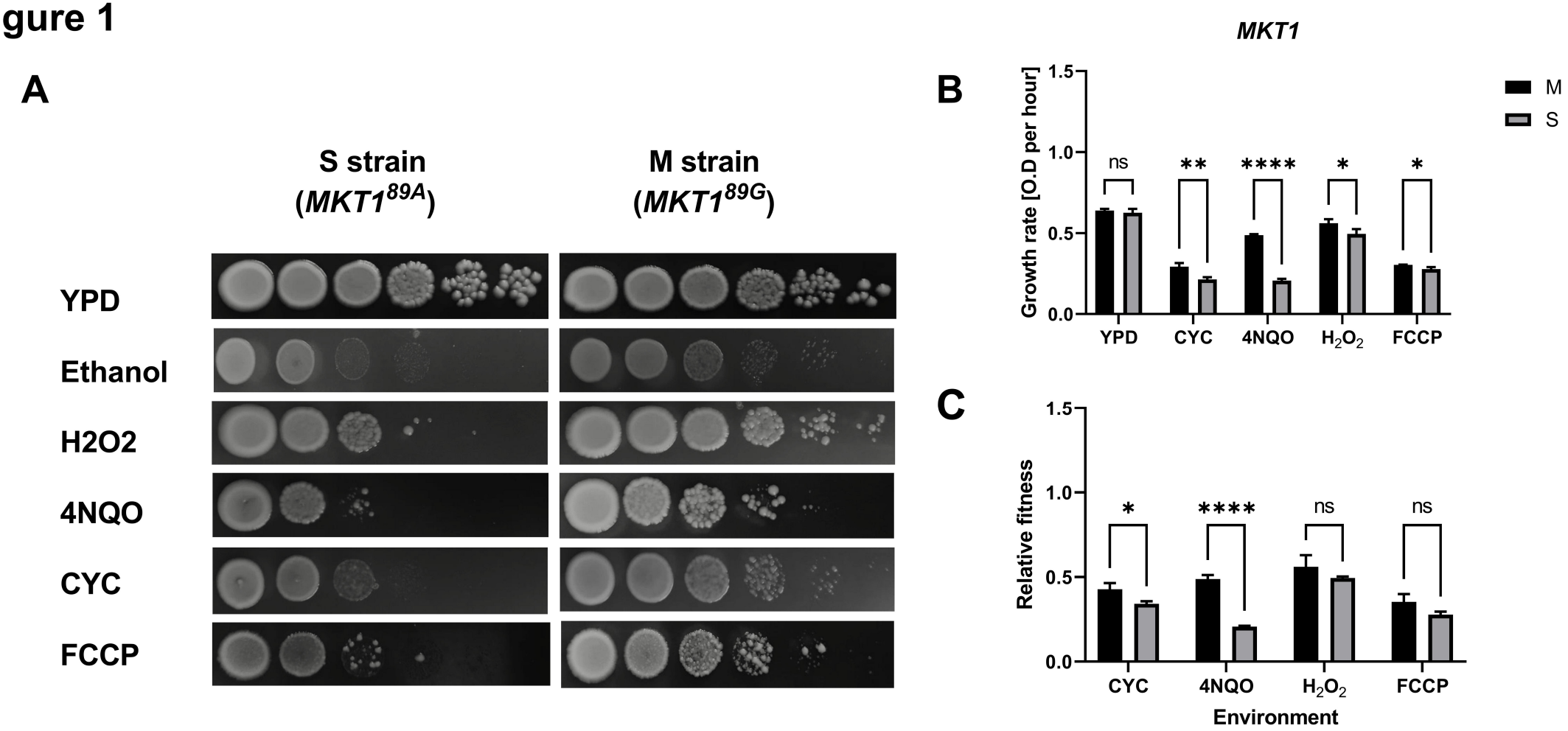
A
S strain
(MKT1 89A)
M strain
(MKT1 89G)
YPD
Ethanol
H2O2
4NQO
CYC
FCCP
B
MKT1
Growth rate [O.D per hour]
1.5
1.0
0.5
0.0
ns
**
****
*
*
YPD
CYC
4NQO
H2O2
FCCP
M
S
C
Relative fitness
1.5
1.0
0.5
0.0
*
****
ns
ns
CYC
4NQO
H2O2
FCCP
Environment

Figure 2

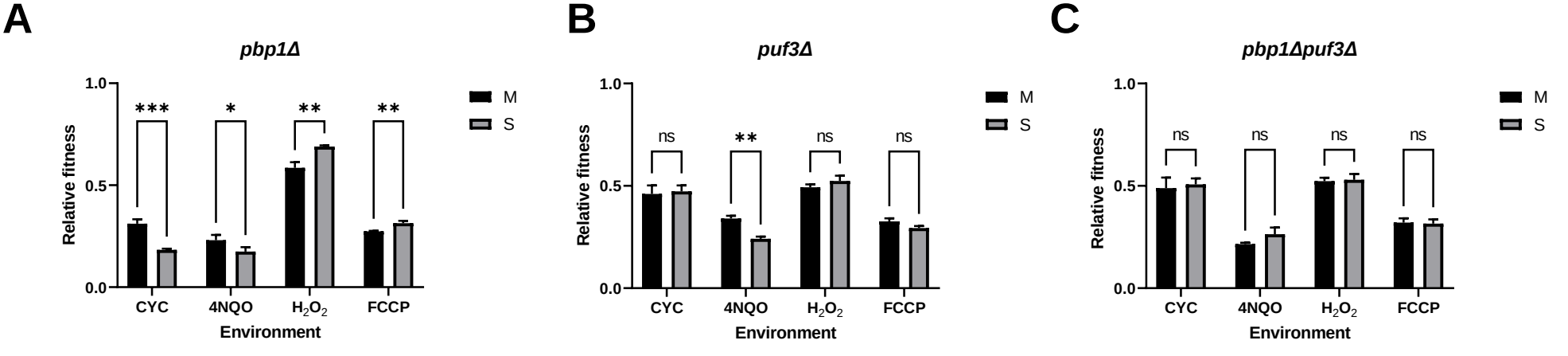
A
pbp1Δ
1.0
0.5
0.0
Relative fitness
***
*
**
**
CYC
4NQO
H2O2
FCCP
Environment
M
S
B
puf3Δ
ns
**
ns
ns
C
pbp1Δpuf3Δ
ns
ns
ns
ns

Figure 3

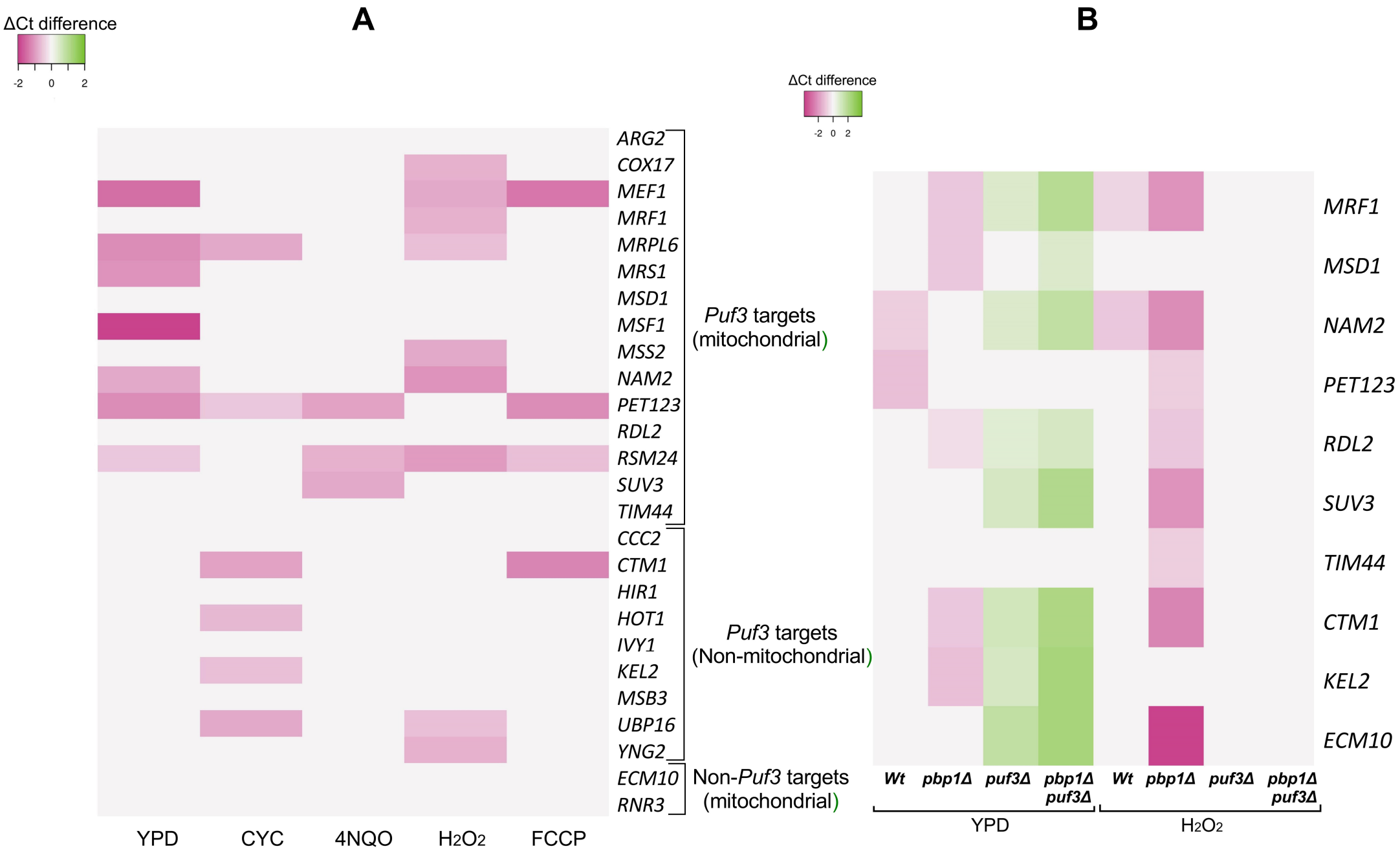
A
ΔCt difference
-2
0
2
ARG2
COX17
MEF1
MRF1
MRPL6
MRS1
MSD1
MSF1
MSS2
NAM2
PET123
RDL2
RSM24
SUV3
TIM44
CCC2
CTM1
HIR1
HOT1
IVY1
KEL2
MSB3
UBP16
YNG2
ECM10
RNR3
Puf3 targets (mitochondrial)
Puf3 targets (Non-mitochondrial)
Non-Puf3 targets (mitochondrial)
YPD
CYC
4NQO
H2O2
FCCP
B
ΔCt difference
-2
0
2
MRF1
MSD1
NAM2
PET123
RDL2
SUV3
TIM44
CTM1
KEL2
ECM10
Wt
pbp1Δ
puf3Δ
pbp1Δ puf3Δ
Wt
pbp1Δ
puf3Δ
pbp1Δ puf3Δ
YPD
H2O2

Figure 4

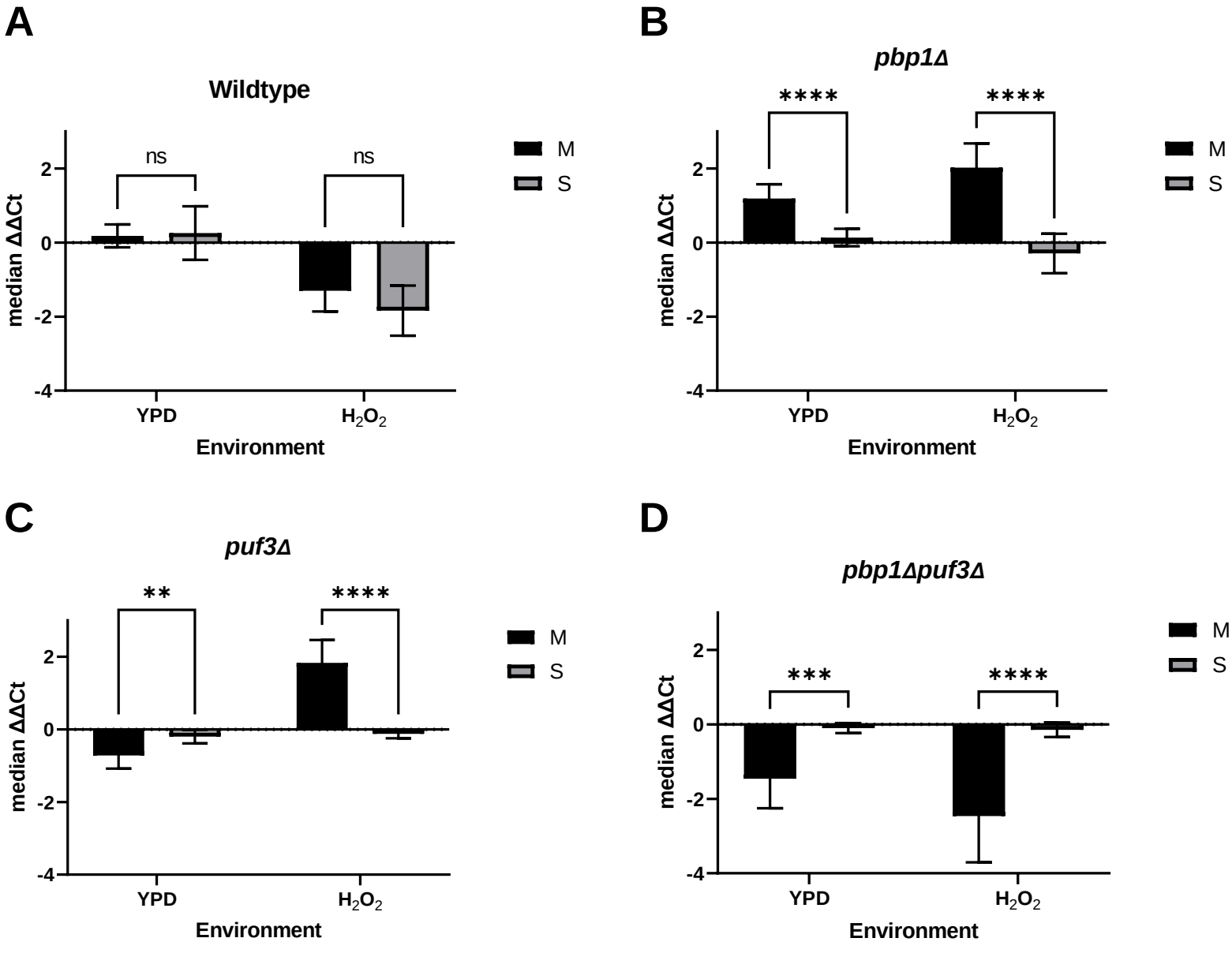
A
Wildtype
ns
ns
M
S
median ΔΔCt
2
0
-2
-4
YPD
H2O2
Environment
B
pbp1Δ
****
****
M
S
median ΔΔCt
2
0
-2
-4
YPD
H2O2
Environment
C
puf3Δ
**
****
M
S
median ΔΔCt
2
0
-2
-4
YPD
H2O2
Environment
D
pbp1Δpuf3Δ
***
****
M
S
median ΔΔCt
2
0
-2
-4
YPD
H2O2
Environment

Figure 5

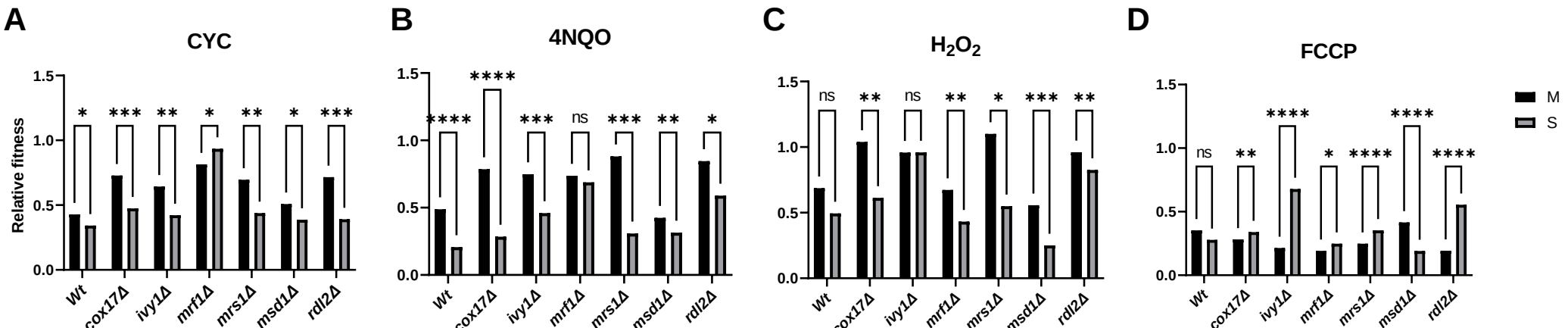
A
CYC
B
4NQO
C
H2O2
D
FCCP
Relative fitness
1.5
1.0
0.5
0.0
Wt
cox17Δ
ivy1Δ
mrf1Δ
mrs1Δ
msd1Δ
rdl2Δ
M
S
ns
*
**
***
****

Figure 6

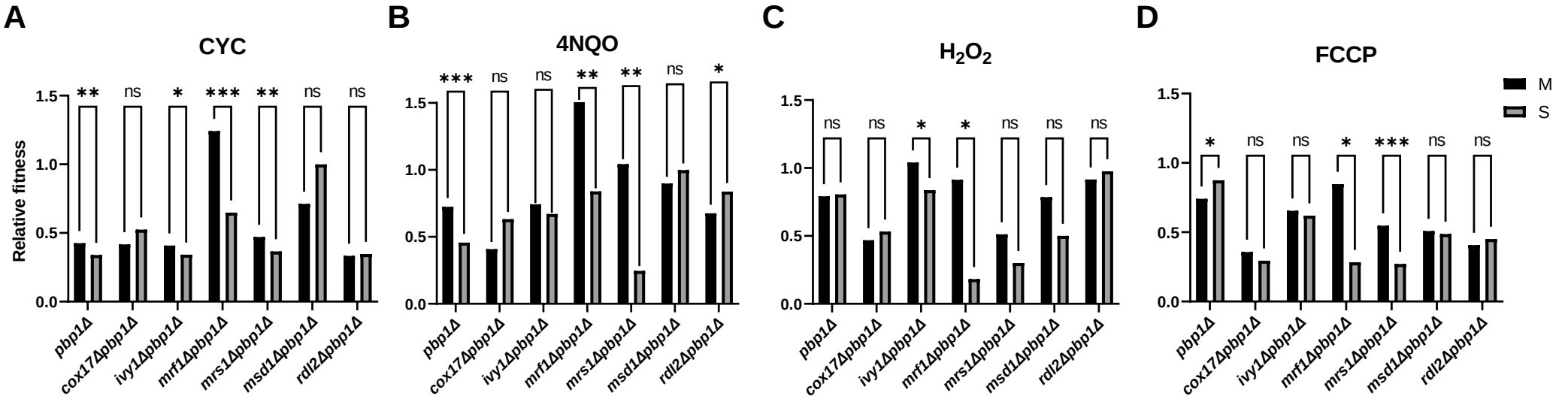
A
CYC
B
4NQO
C
H_2O_2
D
FCCP
M
S
Relative fitness
1.5
1.0
0.5
0.0
**
ns
*
***
**
ns
ns
***
ns
ns
**
**
ns
*
ns
ns
*
*
ns
ns
ns
*
ns
ns
*
***
ns
ns
pbp1Δ
cox17Δpbp1Δ
ivy1Δpbp1Δ
mrf1Δpbp1Δ
mrs1Δpbp1Δ
msd1Δpbp1Δ
rdl2Δpbp1Δ

Figure 7

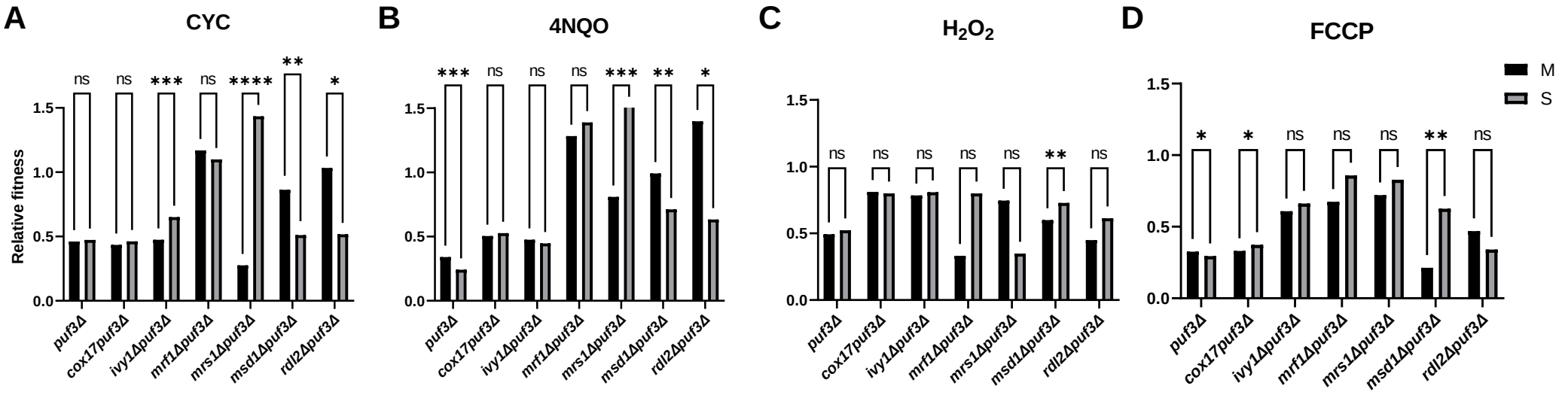
A
CYC
B
4NQO
C
H_2O_2
D
FCCP
M
S
Relative fitness
0.0
0.5
1.0
1.5
ns
*
**
***
****
puf3Δ
cox17puf3Δ
ivy1Δpuf3Δ
mrf1Δpuf3Δ
mrs1Δpuf3Δ
msd1Δpuf3Δ
rdl2Δpuf3Δ

Figure 8

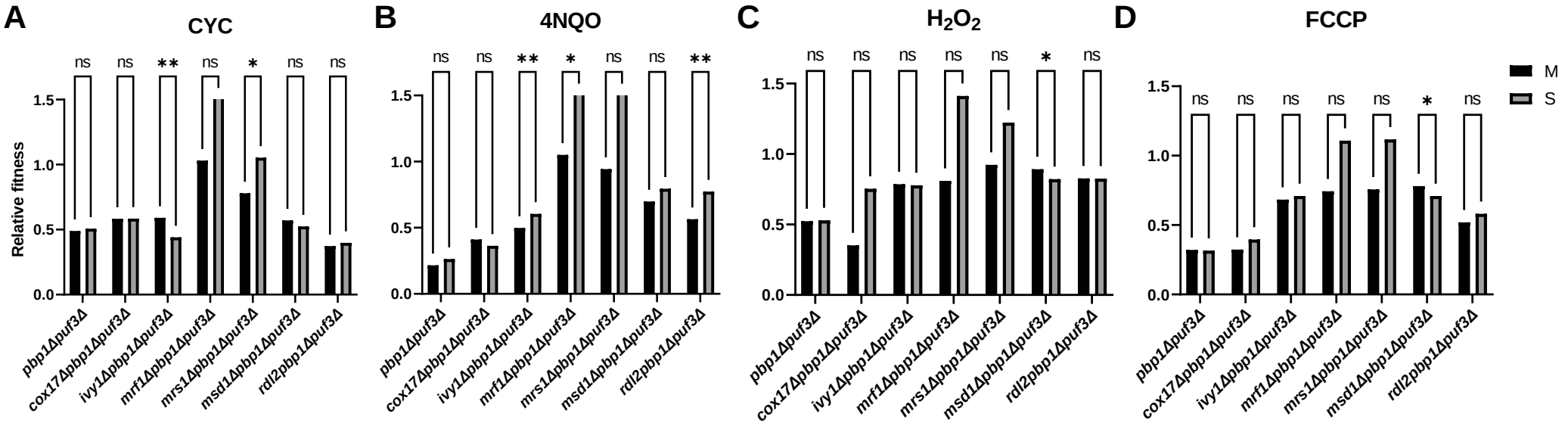
A
CYC
B
4NQO
C
H2O2
D
FCCP
Relative fitness
1.5
1.0
0.5
0.0
ns
**
*
M
S
pbp1Δpuf3Δ
cox17Δpbp1Δpuf3Δ
ivy1Δpbp1Δpuf3Δ
mrf1Δpbp1Δpuf3Δ
mrs1Δpbp1Δpuf3Δ
msd1Δpbp1Δpuf3Δ
rdl2pbp1Δpuf3Δ